Int J Adv Manuf Technol (2011) 53:935–944
DOI 10.1007/s00170-010-2899-5

ORIGINAL ARTICLE

Optimization in thermal friction drilling for SUS 304 stainless steel

Wei-Liang Ku · Ching-Lien Hung · Shin-Min Lee · Han-Ming Chow

Received: 18 May 2010 / Accepted: 15 August 2010 / Published online: 29 August 2010

Abstract The main purpose of this research is to develop a new type of thermal friction drill made of sintered carbide. In addition, to optimize the machining process of the thermal friction drilling using Taguchi method is explored. The experiments were conducted on a 30×30×2 mm SUS 304 stainless steel plate. The effects of friction angles (FA), friction contact area ratio (FCAR), feed rate (FR), and spindle speed (SS) on the two quality characteristics, surface roughness (SR) and bushing length (BL), were also investigated. After conducting all the experimental trials, the analysis procedure followed. Firstly, the significance of the four parameters on the two quality characteristics was examined by ANOVA. Then the optimal combination levels of parameters for SR and BL were determined based on the S/N ratios. Finally, confirmation experiments were conducted to verify the experimental findings. Results showed that FA and SS were the significant machining parameters that most intensively affect SR while FCAR was the only significant parameter for BL. Specially, the SR and BL were greatly improved when used in the optimized parameters settings. More importantly, the performance of the friction drill was conducted 60 runs. The thermal friction drill demonstrated a smoother, mirror-like surface and showed less wear. This proved that thermal friction drilling provided the better machining performance and longer tool life.

Keywords Friction drilling · Friction angle · Friction contact area ratio · Surface roughness · Bushing length · Taguchi method

1 Introduction

Drilling plays a very important role in machining since more than 40% of material removal processes are associated with this type of operation. Traditionally, a drilling tool is usually made of high speed steel (HSS). It generates high temperature during drilling process. Therefore, the drilling tool becomes dull and it leads to a shortened service life. Moreover, the workpiece materials have been hardened during drilling process which makes the post-process troublesome. On the other hand, the chips adhered to the exit of a drilled hole damages the surface quality and deteriorates the machining precision [1]. In order to meet the requirement of excellent tool performance, durability, hardness, and strength, developing a new and versatile

This paper has not been published elsewhere nor has it been submitted for publication elsewhere.

W.-L. Ku (✉)
Department of Information Management,
Nan Kai University of Technology,
Nan Tou 54243 Taiwan, Republic of China
e-mail: t010@nkut.edu.tw

C.-L. Hung
Department of Industrial Engineering and Management,
Nan Kai University of Technology,
Nan Tou, Taiwan, Republic of China

S.-M. Lee
Department of Mechanical Engineering, Army Academy R.O.C.,
Chung-Li, Taiwan, Republic of China

H.-M. Chow
Department of Mechanical Engineering,
Nan Kai University of Technology,
Nan Tou, Taiwan, Republic of China

W.-L. Ku
Department of Industrial Engineering and Management,
National Yunlin University of Science and Technology,
Yunlin 64002 Taiwan, Republic of China

drilling tool is urgent. To define a good drilling tool, the following features should be taken into account: wear-resistance, fracture-resistance, and deformation-resistance.

To overcome the problems above, a tool material coated with a thin TiN layer has been developed to enhance the wear, fatigue, and impact resistance. For example, using a HSS tool coated with TiN can prolong tool life. In addition, the cemented carbide is made from sintering micro-tungsten carbide (WC) particles that would tolerate a high cutting speed near three times larger than that of the HSS [2]. Furthermore, adding TiC or TaC particle to WC–Co matrix can provide a good wear-resistance associated with cemented tungsten carbide. Moreover, the experiments of using WC drills coated with TiN for drilling with stainless plates have been conducted by Lin [3], as the study results found that drilling stainless plates with high speed and feed rate would obtain a large surface roughness and reduce tool life simultaneously. On the other hand, a coolant can be used to cool down the tool temperature in traditional drilling processes. However, it is easy to have impact on human health and work place environment. Hence, traditional wet drilling processes have been replaced by dry drilling processes gradually [4]. Dry drilling usually generated a drilled hole with poor surface quality [5]. Therefore, drilling processes need to consider the following critical issues for improving the drilling characteristics: (1) developing new tool materials for difficult-to-drill materials; (2) developing a novel drilling process to fit the requirements of modern industrial applications; (3) improving tool life, efficiency, and drilled quality; and (4) developing green drilling process without pollution. The most important task of drilling technique is to design a sophisticated drill shape and develop a novel drilling process to fit the requirements of industrial applications.

Thermal friction drilling is a nontraditional drilling method that zealously utilizes the heat generated from the friction interface between a rotating conical tool and the workpiece, and the heat will soften the workpiece and facilitate a drill to penetrate the workpiece plate. Since it was a no-chip process, the surface of the drilled hole would not be damaged by the chip extrusion during the drilling process. Therefore, tool service life could be increased, and the processing elapsed time and drilling cost would be intensively reduced. Another important feature of thermal friction drilling is that it could form a bushing. The bushing can provide a longer contact area which can bear a shaft firmly as well as can be taped to create an internal screw without welding a nut. This is a unique feature which cannot be achieved by common drilling processes.

Referred to thermal friction drilling, there were several papers published recently and reviewed as follows: Kerkhofs [6] conducted the experiments of tungsten carbide coated (Ti, Al) N and indicated that flow drills tool coated carbide could prolong tool life. Miller et al. [7] developed two models for friction drilling. One is the thermal finite element model to predict the distance of tool travel before the workpiece reaches the 250°C threshold temperature that is detectable by an infrared camera. Another is a force model to predict the thrust force and torque in friction drilling based on the measured temperature, material properties, and estimated area of contact. Miller et al. [8] conducted experiments and indicated that materials with different compositions and thermal properties affect the selection of friction drilling process parameters, the surface morphology of the bore, and the development of a highly deformed layer adjacent to the bore surface. Miller et al. [9] suggested that pre-heating the brittle material (cast metals) workpiece and high speed friction drilling process could generate a cylindrical-shaped bushing without significant radial fracture. Miller et al. [10] applied friction drilling to machine low-carbon steel as well as aluminum and magnesium alloys and explored experimentally the relationship between axial thrust force and torque under different spindle speeds and feed rates. However, the effects of tool coating and drilling temperature have not been studied. Lee et al. [11] had successfully applied friction drilling to IN-713LC cast and assessed the material properties after machining including hole roundness as well as surface roughness and hardness of hole wall. Chow et al. [12] conducted experiments using AISI304 stainless steel and indicated that the drilled surroundings area obtained fine grain size and compact structure with a higher micro-hardness than that of the area away from the drilled area. Lee et al. [13] utilized friction drilling to make holes using tungsten carbide drills with and without coating in AISI 304 stainless steel. Their results showed that coated drills suffered less tool wear than uncoated drills at the same spindle speed and for the same number of holes drilled. The above related papers did not explore the optimal parameters combination for friction drilling nor discuss important issues such as geometric shape and cutting parameters affecting drilled hole surface roughness and bushing length, etc.

The Taguchi method is an approach of experimental design and analysis to improve the product quality systematically and powerfully. Recently, the Taguchi method had been widely employed in industrial fields and research works [14–22]. The optimal machining parameters would be established from Taguchi method that transformed the experimental observed values to signal-to-noise (S/N) ratios according to a loss function. The loss function is defined to calculate the deviation between the experimental observed value and the desired value. In general, there are three categories of machining characteristics correlated with the analysis of the S/N ratios, and named as “the higher the better, HB,” “the lower the better, LB,” and “the nominal the better, NB.” Regardless of the category of machining characteristics, the larger S/N ratio means the better machining characteristic.

Following recent technological developments, stainless steel materials with anti-oxidizing, anticorrosive, and shiny surface features and outstanding characteristics like high toughness, high work-hardening coefficient, and low temperature conductivity have been applied in electronic, biochemical, and medical instrumentation equipments. Although these outstanding features reveal the distinguished advantages to extend its applications in modern industries, stainless steel is hard to process and results in a serious tool wear and a rough surface of a part in machining process [15]. The thermal friction drilling presented the potentials of developing a hole drilling with efficiency, high surface quality, and green drilling without environment impact. It was also suitable to any size of drilling process. Therefore, the novel process of the thermal friction drilling needs a further and comprehensive study to understand the effects of drilling performance on stainless steels.

The main purpose of this paper is to present the optimization of machining parameters of the thermal friction drilling process on austenite stainless steel (SUS 304). Moreover, the Taguchi method was adopted to design the experimental study, and the experimental data were statistically surveyed by analysis of variance (ANOVA) for machining characteristics of surface roughness (SR) and bushing length (BL). The significant process parameters affected the SR and BL were determined, and the optimal combination levels of machining parameters were also explored. Thus, the performance of thermal friction drilling process on difficult-to-machine materials such as stainless steel would be ascertained to fit requirements of modern industrial applications.

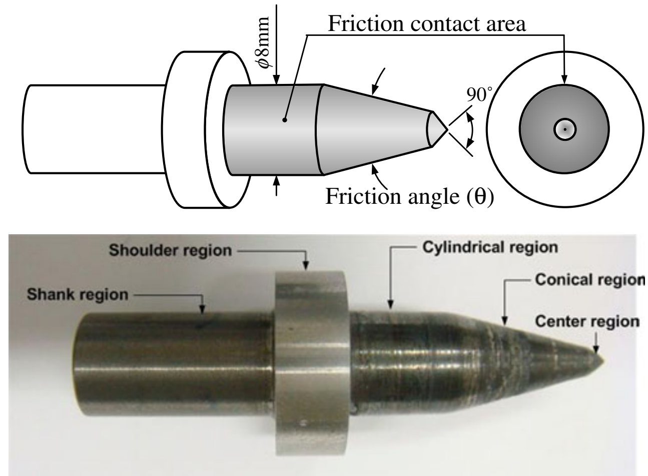

(a) FCAR of 100%

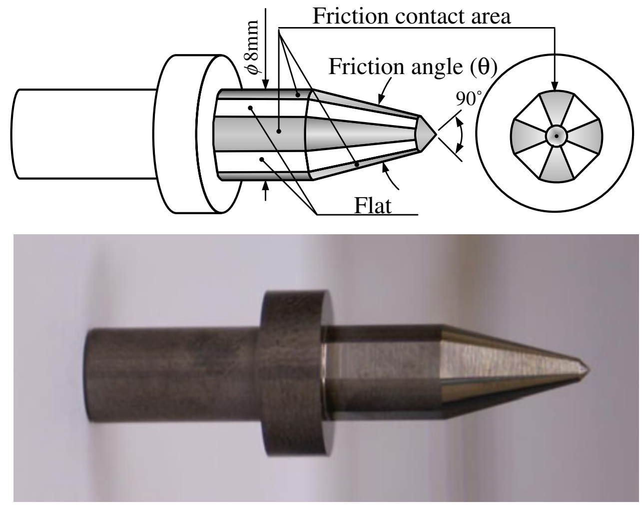

(b) FCAR of 50%

Fig. 1 *Front* and *side views* of thermal friction drill of two different friction contact area ratios (FCARs)

2 Experimental method

2.1 Thermal friction drill design and process mechanism

The thermal friction drill was made by tungsten carbide of cylindrical bar with super fine grain size. The friction drill was ground into conical shape using a diamond grinder shown in Fig. 1a. It showed that the friction contact area ratio (FCAR) is 100%. In order to compare their performance, the drill was ground into a four-leaf: four friction contact areas. The friction contact area for four-leaf was smaller than circumference area; therefore, the FCAR is less 100%. In this case, the FCAR was 50% shown in Fig. 1b. The friction contact area ratio (FCAR) was defined as friction contact area/circumference area. That is, when friction contact area was equal to circumference area, the FCAR is 100%.

Figure 2 demonstrated the thermal friction drilling mechanism using initial type drill. Step 1 described thermal friction drill that penetrated into the specimen using center region of drill with high rotational speed and large thrust force in axle direction initially (see Fig. 1a). Step 2 showed that the molten stainless steel extruded in up-flow using conical region of drill. Step 3 indicated that drill pierces and also extruded the molten stainless steel in down-flow using conical region of drill. Step 4 showed that drill continues to pierce the plate completely using cylindrical region of drill and also extruded from a bushing on the workpiece. Step 5 showed that drill retracted and left a finish hole with a long bushing.

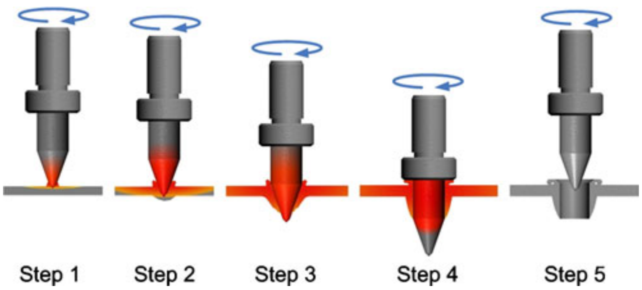

Fig. 2 The schematic illustration of the processing steps for thermal friction drilling

2.2 Material, equipment, and measurement

In this study, the workpiece material was SUS 304 stainless steel plate with the dimension of 30×30×2 mm, and the drilled holes on the plate had a diameter of 8 mm made using a CNC machine center (Fulland FMC-1000). This study utilized the friction drilling conditions as 1,200~3,600 rpm drilling speed and 75~125 mm/min feed rate (refers to SANDVIK tool handbook) to conduct the experiments. The chemical composition of SUS 304 stainless steel was shown in Table 1.

Figure 3 showed a schematic diagram of the experimental setup for friction drilling. The thermal friction drill was made of tungsten carbide (WC) with conical shape as presented in Fig. 1. The value of SR was obtained from averaging five measurements stochastically conducted on different positions of cross section using precision profilometry. In order to measure the bushing length, CNC wire cutter was used to cut the workpiece on the center line that formed a cross section, the bushing length was calculated from the top edge to the bottom serrated edges of the workpiece, and the serrated edges were cut off. The bushing length (BL) was measured by a tool-maker microscope, and the surface topographies of drilled holes were observed by a scanning electron microscope (SEM) to inspect their surface integrity.

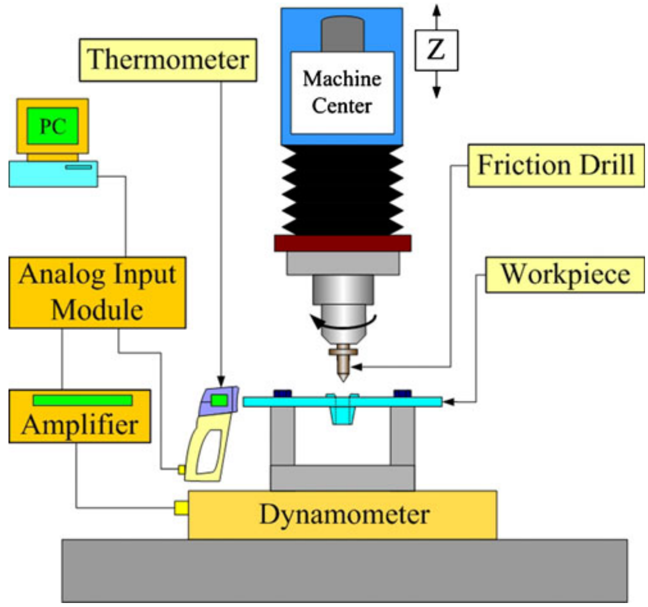

Fig. 3 Experimental setup of thermal friction drilling

2.3 Experimental design based on Taguchi method

In this study, an orthogonal array L9 based on Taguchi method was applied to design the experiments. Using the Taguchi orthogonal array to conduct the experiment markedly reduced the number of experiments, and the process parameters were systematically and comprehensively explored. The experimental observed values and the levels of the process parameters were shown in Table 2.

Two observed characteristics such as surface roughness (SR) and bushing length (BL) were examined. The levels of each process parameter were set in accordance with the L9 orthogonal array based on the Taguchi experimental design method. The S/N ratios were calculated from observed values. In this investigation, the experimentally observed value SR was "the lower the better" while and the value of BL was "the higher the better." Therefore, the optimal

Table 1 Chemical composition of SUS 304 stainless steel

Chemical element	Content (%)
C	0.08
Si	1.0
Mn	2.0
P	0.045
S	0.03
Cr	18–20
Ni	8–12

Table 2 Experimental observed characteristics and levels of machining parameters

Observed characteristics	Control parameters	Levels		
• Surface roughness, SR (μm)	Friction Angle, FA (Degree)	30	45	60
	Friction contact area ratio, FCAR (%)	50	75	100
• Bushing length, BL (mm)	Feed rate, FR (mm/min)	75	100	125
	Spindle speed, SS (rpm)	1,200	2,400	3,600

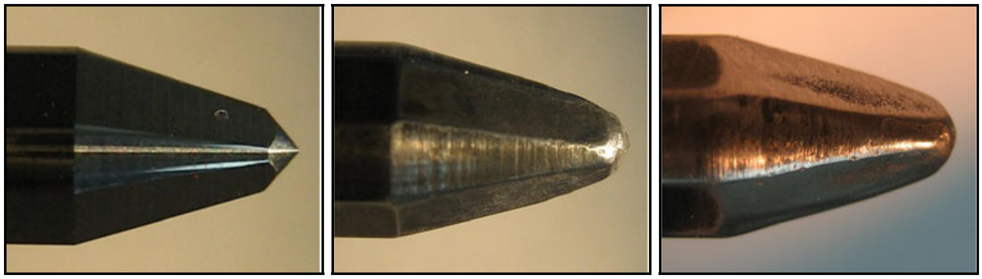

Fig. 4 Thermal friction drills before and after drilling the SUS 304 stainless steel

observed SR was its minimum value, and the optimal BL was the maximum value. Small SR value means better surface roughness and large BL means firmer contact between hole and shaft of parts. However, the characteristics of the S/N ratios for SR and BL were always "the higher the better." Both "the higher the better" and "the lower the better" calculations were given in the following equations [15–19, 22].

The higher the better characteristic : (1)

$$\eta = -10\log\left[\frac{1}{n}\sum_{i=1}^{n} y_i^{-2}\right]$$

The lower the better characteristic : (2)

$$\eta = -10\log\left[\frac{1}{n}\sum_{i=1}^{n} y_i^{2}\right]$$

where η denotes the S/N ratio calculated from observed values (unit: db); y_i represents the experimentally observed value of the ith experiment, and n is the repeated number of each experiment. Notably, each experiment in the L9 array is conducted three times.

The S/N ratios determined from experimental observed values were statistically studied by ANOVA to explore the effects of each machining parameter on the observed values and to elucidate which machining parameters significantly affected the observed values. The related equations are as follows:

$$S_m = \frac{\left(\sum \eta_i\right)^2}{9} \tag{3}$$

$$S_T = \sum \eta_i^2 - S_m \tag{4}$$

$$S_A = \frac{\sum \eta_{Ai}^2}{N} - S_m \tag{5}$$

$$V_A = \frac{S_A}{f_A} \tag{6}$$

where

- S_m is the sum of squares, based on the mean.
- S_T is the sum of squares, based on the total variation.
- S_A is the sum of squares, based on parameter A (for example, A=FA, FCAR, FR, and SS).
- η_i is the value of η in the ith experiment (i=1–9).
- η_{Ai} is the sum of the ith level of parameter A (i=1,2,3).
- N is the repeating number of each level of parameter A.
- f_A is the number of degrees of freedom of parameter A.
- V_A is the variance of parameter A.

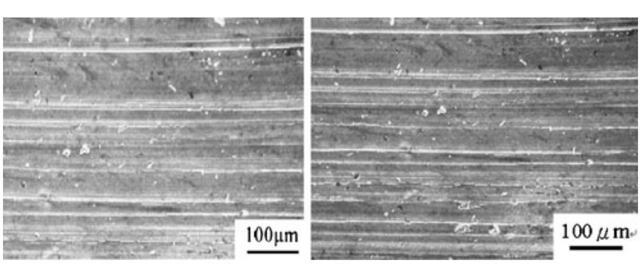

Fig. 5 SEM micrographs of the machined hole surfaces obtained after 30 and 60 runs of friction drilling

Table 3 L9 orthogonal array, control parameters, and S/N ratios

No.	Control parameters				S/N ratios (η)	
	FA	FCAR	FR	SS	SR	BL
1	30	50	75	1,200	−6.3613	15.0563
2	30	75	100	2,400	−0.9844	14.2193
3	30	100	125	3,600	−4.5062	12.7498
4	45	50	100	3,600	−2.6708	14.5995
5	45	75	125	1,200	−13.1028	14.4527
6	45	100	75	2,400	−7.0050	13.8216
7	60	50	125	2,400	−8.4321	15.4023
8	60	75	75	3,600	−6.5267	14.9947
9	60	100	100	1,200	−10.6296	14.0141

Table 4 ANOVA of surface roughness (SR)

Parameter (A)	Degree (f_A)	Square sum (S_A)	Variance (V_A)	Contribution (%)
FA	2	35.1090	17.5545	30.96[a]
FCAR	2	3.7914	1.8957	3.34
FR	2	23.0514	11.5257	20.33
SS	2	51.4384	25.7192	45.36[a]
Total	8	113.3901	56.6951	100.00

[a] Significant parameter: contribution more than 25%

2.4 Experimental conditions

The effects of machining parameters on machining characteristics were extensively investigated in this study. Moreover, the significant parameters and the optimal combination levels of machining parameters were determined. The main machining parameters: friction angle (FA), friction contact area ratio (FCAR), feed rate (FR), and spindle speed (SS), were varied to determine their effects on the machining characteristics SR and BL. The S/N ratios were calculated from the experimental observed values, according to Eqs. 1 and 2. The optimal combination levels of the machining parameters that produced low SR and high BL were determined by analyzing the S/N ratios. In addition, the significant machining parameters associated with SR and BL were also examined by ANOVA.

3 Results and discussions

3.1 The features of thermal friction drilling process

The SUS 304 stainless steel has great toughness, low thermal conductivity, and high work-hardening coefficient. Therefore, stainless steel is hard to process and results in a serious and quick tool wear and a rough surface of a part in machining [15]. This experiment employed self-made friction drill to conduct continual and long time drillings (60 runs) on SUS 304 stainless steel. Mainly, the experiments are to observe tool wear and drilled hole surface. However, the thermal friction drill could drill the SUS 304 stainless steel after 30 runs almost without wear of drill. Furthermore, it only generated a little wear and was able to keep on drilling process after 60 runs (see Fig. 4).

Figures 5a and b showed the SEM micrographs of two machined holes after 30 runs and 60 runs of friction drilling. From the two micrographs observations, we found that their drilled surfaces were very uniform and smooth due to the following reasons: (1) there was little drill wear for both 30 and 60 runs and (2) thermal friction drilling utilized the heat generated from friction between a conical tool and the workpiece to soften and penetrate a sheet metal and formed a hole without sharp edge to tear and cut material.

In summary, the thermal friction drill efficiently utilized the heat factor that was created from friction between drill and workpiece. The tool penetrated more easily after workpiece softening. Moreover, the friction drill would be prevented from wearing quickly because it exhibited an extensive short drilling time (a hole is drilled typically for only 8 s). Therefore, the thermal friction drilling process enhanced the surface quality of the drilled hole and prolonged the tool service life more significantly.

3.2 The effects of thermal friction drilling process on surface roughness (SR)

Table 3 showed the S/N ratios of SR and BL. According to the L9 orthogonal array, each experimental setting was also listed in this table. Table 4 showed the contribution of each machining parameter for SR. Data were calculated from the S/N ratio of variance associated with each machining

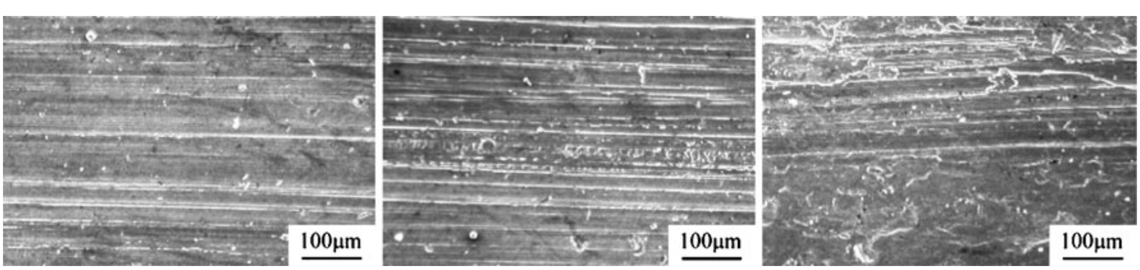

(a) FA=30º (b) FA=45º (c) FA=60º

Fig. 6 SEM micrographs of the machined hole surfaces obtained with various friction angles (FA)

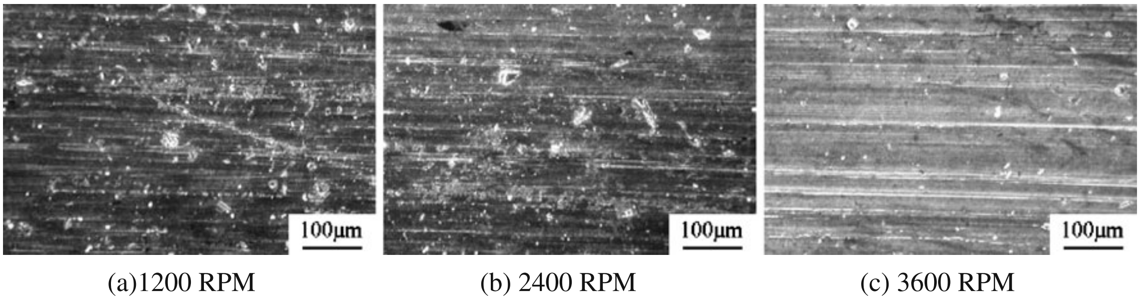

Fig. 7 SEM micrographs of the machined hole surfaces obtained with various spindle speeds (when feed rates=100 mm/min)

parameter. The statistical analysis results showed that the FA and the SS were the significant machining parameters of thermal friction drilling, which would obviously affect the SR. When the friction angle was set at small level (FA=30°), the contact length (i.e., the length of conical region) of a thermal friction drill was longer. Therefore, a higher and uniform melting temperature would be generated on the drilling surface. Consequently, a small SR was obtained from the wall of drilled hole (see Fig. 6a), as the thermal friction drill pierced the specimen plate. However, when the friction angle increased gradually and the contact length became shorter, a lower and uneven temperature field would be produced during the thermal friction drill performing on the workpiece. As a result, scratch marks would reveal on the surface of drilled hole when the thermal drill pierced through the workpiece. Therefore, a large value of SR would be obtained (see Fig. 6c).

Secondly, when spindle speed (SS) increased from 1,200 to 3,600 rpm, the amount of heat energy was enlarged in a moment due to high speed friction between drill and part. The high heat energy would soften the stainless steel and increase the tool cutting capability. Thus, better surface quality of a drilled hole was obtained. Figure 7 showed the SEM micrographs of the drilled hole surfaces under various SS, as this figure showed that the drilled hole of 3,600 rpm revealed the most finishing and smooth surface integrity. Figure 8 depicted the S/N ratios response graph of SR. From this plot, the optimal combination levels of the machining parameters on SR correlated to thermal friction drilling would be obtained. As shown in this figure, the optimal machining parameter levels on SR were as follows: FA=30°, FCAR=50%, FR=100 mm/min, and SS=3600 RPM.

3.3 The effects of thermal friction drilling process on bushing length (BL)

Table 5 lists the ANOVA and the contribution of each machining parameter for the experimental observed value of BL. As the analysis results show that the FCAR is the significant parameter for generating the maximum BL during the thermal friction drilling. Since the thermal friction would soften the stainless plate and enhance the fluidity of plastic material on the drilling area, the ductile

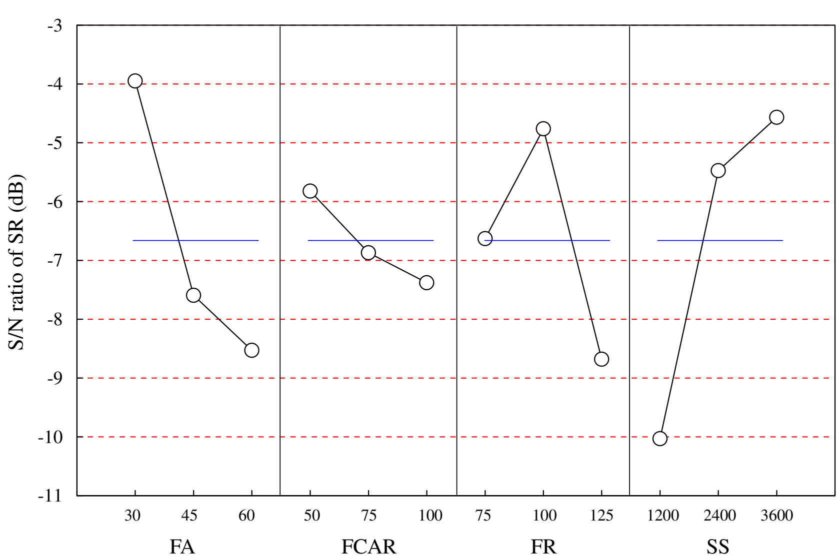

Fig. 8 Response graph of S/N ratios for surface roughness (SR)

Table 5 ANOVA of bushing length (BL)

Parameter (A)	Degree (f_A)	Square sum (S_A)	Variance (V_A)	Contribution (%)
FA	2	1.0207	0.5103	20.30
FCAR	2	3.4064	1.7032	67.76[a]
FR	2	0.2958	0.1479	5.88
SS	2	0.3045	0.1522	6.06
Total	8	5.0274	2.5137	100.00

[a] Significant parameter: contribution more than 25%

stainless plate was pierced through easily and fast at elevated temperature. Indeed, the friction drill with four leaves will work on a continual contact and generate the intermittent stirring effect on the hole wall of workpiece during drilling. Therefore, the intermittent stirring effect and feed rate of tool spindle direction will prolong the bushing length. Thus, small FCAR would enhance the fluidity of the softened material to obtain a longer BL. Figure 9 showed the photographs of the bushings under various FCAR, and this figure also showed that the friction drill of 50% FCAR generated a longer BL. Figure 10 depicts the S/N ratios response graph of BL; the optimal combination levels of machining parameters for BL were as follows: FA=60°, FCAR=50%, FR=75 mm/min, and SS= 1,200 rpm.

3.4 Confirmation experiments

The optimal combination levels of machining parameters were determined and confirmed in the following. The estimated S/N ratios are calculated as:

$$\widehat{\eta} = \overline{\eta}m + \sum_{i=1}^{n_o} (\overline{\eta}i - \overline{\eta}m) \tag{7}$$

$\widehat{\eta}$ estimated S/N ratio for optimal combination levels of machining parameters.
$\overline{\eta}m$ total mean S/N ratio.
n_0 the number of significant parameters.
$\overline{\eta}i$ mean S/N ratio at the optimal level.

Table 6 displays the results of the confirmation experiments. This table indicated that the S/N ratios associated with SR and BL for the optimal combination levels of machining parameters are 8.09 and 1.14 db which were greater than those obtained under the initial experimental conditions: FA (45°), FCAR (75%), FR (100 mm/min), and SS (2,400 rpm). Therefore, the experimental results confirmed that the machining parameters would be optimized for each machining characteristic and the observed values would thus be significantly improved.

Figure 11 showed the top view and cross section of a drilled hole using the optimal parameters. From the hole cross section, the BL of the drilled hole was near three times of the specimen thickness. The bushing provided a longer contact area which can sustain a shaft firmly, and the hole surface was smooth like a mirror (Ra=0.96 μm). In general, the measured diameters of drilled holes presented variations in a range of about ±0.01 mm. The diameter of hole was almost similar to the diameter of drill. Expansion of the hole was rarely found in this study. Therefore, it can be employed to serve as a cylindrical sleeve bearing. Moreover, it could be taped to create an internal screw without especially welding a nut on the plate under the machined hole shown in Fig. 12. It extensively reduced the complicated procedures of joining components in the aerospace and automotive industries.

4 Conclusions

This study investigated the thermal friction drilling effects on SR and BL based on Taguchi methodology for SUS304 stainless steel. Experimental data and statistical results support the following conclusions:

(1) The thermal friction drill efficiently utilized the heat factor that was created from the friction between a drill

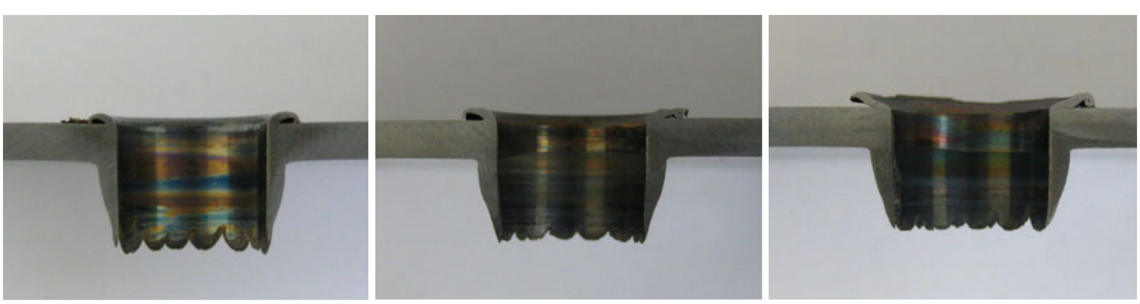

FCAR: 50% FCAR: 75% FCAR: 100%

Fig. 9 Photographs of the bushing length (BL) obtained from various friction contact area ratios (FCARs; under the condition of FA=60°, FR= 100 mm/min, and SS=1,200 rpm)

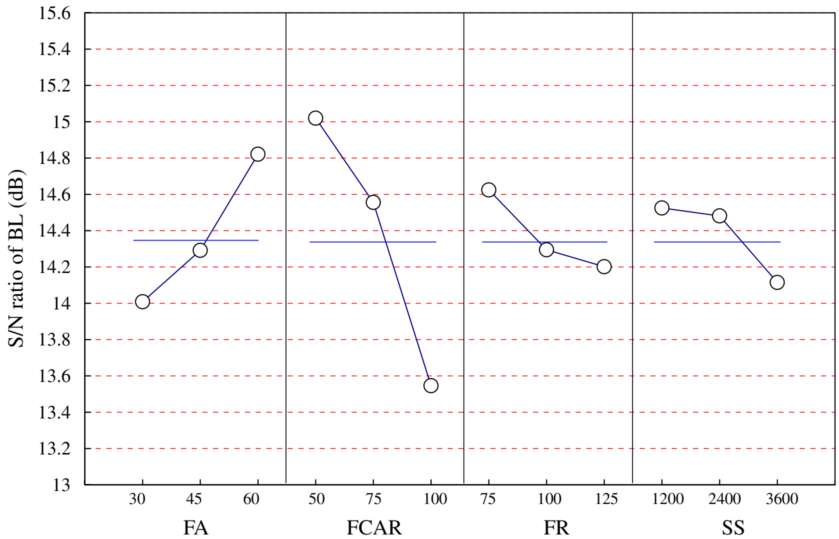

Fig. 10 Response graph of S/N ratios for bushing length (BL)

and a workpiece, and then drill penetrated more easily after the workpiece was softened. Moreover, since the friction drill was prevented from wearing quickly, this meant the drilling time was short. Simultaneously, thermal friction drilling avoided serious tool wear and prolonged the tool service life. The surface quality of the drilled hole was also improved significantly.

(2) Under the optimal friction drilling condition, the bushing length (BL) of the drilled hole was near three times longer than the plate thickness which BL was used as a sustain area for a shaft and taped as an internal screw for joining components on the plate. Moreover, the wall surface of the drilled hole revealed a mirror-like quality (Ra=0.96 μm).

(3) The friction angle (FA) and the spindle speed (SS) were the significant machining parameters, which obviously affected surface roughness (SR) in thermal friction drilling. Moreover, the optimal machining parameter levels on SR were FA=30°, FCAR=50%, FR=100 mm/min, and SS=3,600 rpm. Because when the FA was small (30^{o}) and the contact length (i.e., the length of conical region) was longer, the drilled workpiece would generate a higher and even melting temperature. Simultaneously, when the SS increased from 1,200 to 3,600 rpm, the amount of heat energy was enlarged in a moment due to high speed friction between drill and part. The high heat energy softened the stainless steel and increased the tool cutting capability. Thus, better surface quality of a drilled hole was obtained.

(4) The friction contact area ratio (FCAR) was the only significant parameter for bushing length (BL) during thermal friction drilling. Because when the FCAR of 50% was applied, the friction drill with four leaves worked on a continual contact and generated the

Table 6 Results of the confirmation experiments

Observer values	Initial levels of machining parameters	Optimal combination levels of machining parameters	
	$A_2B_2C_2D_2$	Prediction	Experiment
S/N ratio (dB) for SR	−9.07	−1.83	−0.98
S/N ratio (dB) for BL	14.01	15.02	15.15

(a) Top view of hole bushing

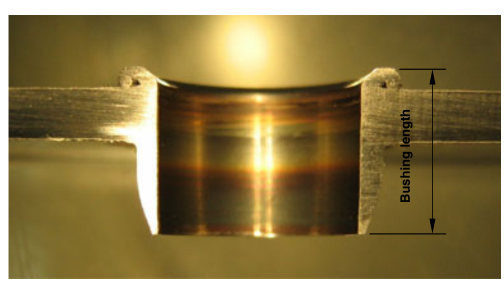

(b) Cross section of hole bushing

Fig. 11 Top view and cross section of a drilled hole bushing using the optimal parameters (FA=30°, FCAR=50%, FR=100 mm/min, SS=3,600 rpm)

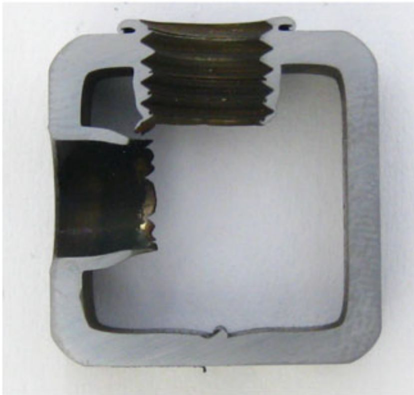

Cross section of internal screw

Fig. 12 An internal screw without especially welding a nut on the square tube

intermittent stirring effect on the hole wall of workpiece during drilling. Therefore, the intermittent stirring effect and feed rate of tool spindle direction prolonged the bushing length. Therefore, the optimal combination levels of machining parameters for BL were FA=60°, FCAR=50%, FR=75 mm/min, and SS=1200 RPM.

(5) The S/N ratios of the optimal combination levels of thermal friction drilling parameters determined according to Taguchi method were 8.09 and 1.14 db greater than those obtained under the initial experimental conditions (FA=45°, FCAR=75%, FR=100 mm/min, and SS=2,400 rpm) for SR and BL individually. The machining characteristics of thermal friction drilling on 2 mm SUS 304 stainless plate were improved obviously.

(6) This study can be applied on the friction drilling of various malleable metals including mild steel, stainless steel, cooper, brass, and aluminum to generate precision holes with bushing formed underside. The bushing can serve as a sleeve bearing, a location for a brazed connection, or tapping to give deep screw threads. Friction drilled parts can also be used in domestic (electric) appliances and bike skeleton, etc.

Acknowledgment The authors would like to thank the National Science Council of the Republic of China for financially supporting this research under Contract No. NSC 97-2221-E-252-004.

References

1. Cantero JL, Tardío MM, Canteli JA, Marcos M, Miguélez MH (2005) Dry drilling of alloy Ti-6Al-4V. Int J Mach Tools Manuf 45:1246–1255
2. Noordin MY, Venkatesh VC, Sharif S (2007) Dry turning of tempered martensitic stainless tool steel using coated cermet and coated carbide tools. J Mater Process Technol 185:83–90
3. Lin T-R (2002) Cutting behavior of a TiN-coated carbide drill with curved cutting edges during the high-speed machining of stainless steel. J Mater Process Technol 127:8–16
4. Nouari M, List G, Girot F, Géhin D (2005) Effect of machining parameters and coating on wear mechanisms in dry drilling of aluminium alloys. Int J Mach Tools Manuf 45:1436–1442
5. Bono M, Jun N (2001) The effects of thermal distortions on the diameter and cylindricity of dry drilled holes. Int J Mach Tools Manuf 41:2261–2270
6. Kerkhofs M, Van Stappen M (1994) The performance of (Ti, Al) N-coated flow drills. Surf Coat Technol 68(69):741–746
7. Miller SF, Blau PJ, Shih AJ (2005) Microstructural alterations associated with friction drilling of steel, aluminum, and titanium. J Mater Eng Perform 14:647–653
8. Miller SF, Li R, Wang H, Shih AJ (2006) Experimental and numerical analysis of the friction drilling process. Transactions of the ASME 128:802–810
9. Miller SF, Tao J, Shih AJ (2006) Friction drilling of cast metals. Int J Mach Tools Manuf 46:1526–1535
10. Miller SF, Blau PJ, Shih AJ (2007) Tool wear in friction drilling. Int J Mach Tools Manuf 47:1636–1645
11. Lee SM, Chow HM, Yan BH (2007) Friction drilling of IN-713LC cast superalloy. Mater Manuf Processes 22:893–897
12. Chow HM, Lee SM, Yang LD (2008) Machining characteristic study of friction drilling on AISI 304 stainless steel. J Mater Process Technol 207:180–186
13. Lee SM, Chow HM, Huang FY, Yan BH (2009) Friction drilling of austenitic stainless steel by uncoated and PVD AlCrN- and TiAlN-coated tungsten carbide tools. Int J Mach Tools Manuf 49:81–88
14. Bagci E, Ozcelik B (2006) Analysis of temperature changes on the twist drill under different drilling condition based on Taguchi method during dry drilling of Al 7075-T651. Int J Adv Manuf Technol 29:629–636
15. Yang LD, Lin CT, Chow HM (2009) Optimization in MAF operations using Taguchi parameter design for AISI304 stainless steel. Int J Adv Manuf Technol 42:595–605
16. Lin YC, Yan BH, Huang FY (2001) Surface improvement using a combination electrical discharge machining with ball burnish machining based on the Taguchi method. Int J Adv Manuf Technol 18:673–682
17. Lin C-T, Yang LD, Chow HM (2007) Study of magnetic abrasive finishing in free-form surface operations using the Taguchi method. Int J Adv Manuf Technol 34:122–130
18. Kurt M, Bagci E, Kaynak Y (2009) Application of Taguchi methods in the optimization of cutting parameters for surface finish and hole diameter accuracy in dry drilling processes. Int J Adv Manuf Technol 40:458–469
19. Deng CS, Chin JH (2005) Hole roundness in deep hole drilling as analysed by Taguchi methods. Int J Adv Manuf Technol 25:420–426
20. Gaitonde VN, Kamik SR, Achyutha BT, Siddeswarappa B (2007) Methodology of Taguchi optimization for multi-objective drilling problem to minimize burr size. Int J Adv Manuf Technol 34:1–8
21. Jain NK, Jain VK, Jha S (2007) Parametric optimization of advanced fine-finishing processes. Int J Adv Manuf Technol 34:1191–1213
22. Bagci E, Aykut S (2006) A study of Taguchi optimization method for identifying optimum surface roughness in CNC face milling of cobalt-based alloy (stellite 6). Int J Adv Manuf Technol 29:940–947